


## Article

# Effect of Salinity on UVA-Vis Light Driven Photo-Fenton Process at Acidic and Circumneutral pH

Iván Vallés<sup>1</sup>, Lucas Santos-Juanes<sup>1</sup>, Ana M. Amat<sup>1</sup>, Javier Moreno-Andrés<sup>2</sup>  and Antonio Arques<sup>1,\*</sup>

<sup>1</sup> Grupo de Procesos de Oxidación Avanzada, Departamento de Ingeniería Textil y Papelera, Universitat Politècnica de València, Campus de Alcoy, 03801 Alcoy, Spain; iwalfes@epsa.upv.es (I.V.); lusanju1@txp.upv.es (L.S.-J.); aamat@txp.upv.es (A.M.A.)

<sup>2</sup> Department of Environmental Technologies, Faculty of Marine and Environmental Sciences, INMAR-Mrine Research Institute, CEIMAR-International Campus of Excellence of the Sea, University of Cadiz, Campus Universitario de Puerto Real, 11510 Cádiz, Spain; javier.moreno@uca.es

\* Correspondence: aarques@txp.upv.es

**Abstract:** In the present work, the treatment of a mixture of six emerging pollutants (acetamiprid, acetaminophen, caffeine, amoxicillin, clofibric acid and carbamazepine) by means of photo-Fenton process has been studied, using simulated sunlight as an irradiation source. Removal of these pollutants has been investigated in three different aqueous matrices distinguished by the amount of chlorides (distilled water, 1 g L<sup>-1</sup> of NaCl and 30 g L<sup>-1</sup> of NaCl) at a pH of 2.8 and 5.0. Interestingly, the presence of 1 g L<sup>-1</sup> was able to slightly accelerate the pollutants removal at pH = 5, although the reverse was true at pH = 2.8. This is attributed to the pH-dependent interference of chlorides on photo-Fenton process, that is more acute in an acidic medium. As a matter of fact, the fastest reaction was obtained at pH = 3.5, in agreement with literature results. Monitoring of hydrogen peroxide consumption and iron in solution indicates that interference with chlorides is due to changes in the interaction between iron and the peroxide, rather than a scavenging effect of chloride for hydroxyl radicals. Experiments were also carried out with real seawater and showed higher inhibition than in the NaCl experiments, probably due to the effect of different dissolved salts present in natural water.

**Keywords:** photo-Fenton; wastewater; chlorides; simulated sunlight; pH effect



**Citation:** Vallés, I.; Santos-Juanes, L.; Amat, A.M.; Moreno-Andrés, J.; Arques, A. Effect of Salinity on UVA-Vis Light Driven Photo-Fenton Process at Acidic and Circumneutral pH. *Water* **2021**, *13*, 1315. <https://doi.org/10.3390/w13091315>

Academic Editor: Stefanos Giannakis

Received: 13 April 2021

Accepted: 3 May 2021

Published: 8 May 2021

**Publisher's Note:** MDPI stays neutral with regard to jurisdictional claims in published maps and institutional affiliations.

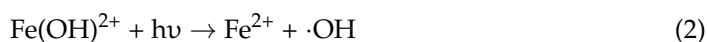
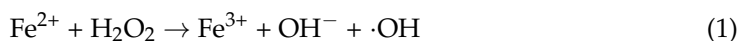


**Copyright:** © 2021 by the authors. Licensee MDPI, Basel, Switzerland. This article is an open access article distributed under the terms and conditions of the Creative Commons Attribution (CC BY) license (<https://creativecommons.org/licenses/by/4.0/>).

## 1. Introduction

Advanced oxidation processes (AOPs) have been demonstrated as a good alternative to treat pollutants which cannot easily removed by classical processes. Among them contaminants of emerging concern (CEC) can be found, which are released to the environment at relatively low concentrations as a consequence of human activity [1,2]. Some of the AOPs employed to treat CECs are photochemical, such as UV photolysis, photocatalysis with semiconductors such as TiO<sub>2</sub> or the photo-Fenton process [2,3].

The photo-Fenton process consists in the ability of iron salts to catalyze the decomposition of hydrogen peroxide into highly reactive species, among them, the hydroxyl radical ( $\cdot\text{OH}$ ) [4]. Briefly, iron (II) reacts with H<sub>2</sub>O<sub>2</sub> to generate  $\cdot\text{OH}$ , but it is oxidized to Fe(III) according to Equation (1). The regeneration of Fe(II) is the limiting step, and strategies are needed to accelerate it. For instance, the process is highly enhanced by light according to Equation (2) and as photons with a wavelength below 500 nm can drive the reaction, sunlight can be employed for this purpose [5]. However, the mechanism of (photo)-Fenton is very complex and it remains to be completely elucidated; other reactions can also take place.



As  $\text{Fe}(\text{OH})^{2+}$  is the key species in the process, it is clear that iron speciation and complexation of this cation can strongly modify the efficiency of photo-Fenton. For instance, it is widely described that the optimum pH value for the Fenton process is 2.8, and beyond this point, a significant loss of efficiency can be observed [6]. This is attributable to the formation of other species instead of  $\text{Fe}(\text{OH})^{2+}$  when the concentration of  $\text{OH}^-$  increases (first  $\text{Fe}(\text{OH})_2^+$ , then other iron oxides and hydroxides), which are not able to drive Equation (2), and hence the catalytic cycle of iron is not closed, with a concomitant loss of efficiency in the generation of reactive species.

In addition, other species present in the aqueous mixture might have a strong influence on the photo-Fenton process. On one side, the presence of some anions such as phosphate, chloride or carbonate have been described to inhibit photo-Fenton [7]. While the first one forms iron phosphate, a very stable and insoluble salt that decreases iron availability, the presence of which is incompatible with Fenton chemistry [8], the other ions interact with iron, modifying the Fenton mechanism and generating less reactive species that limit but do not stop the Fenton process [9–11].

On the contrary, some organic compounds and macromolecules are able to form iron complexes, which in some cases can close the catalytic cycle, in which Equation (3) replaces Equation (2). This ability to form stable chelates can prevent the formation of inactive iron species at increasing pH, and hence, it has been employed in strategies aiming to extend the applicability of photo-Fenton to milder pH domains [6]. In this context, carboxylic acids [12], phenolic substances [13], ethylenediamine- $N,N'$ -disuccinic acid, EDDS or ethylenediaminetetraacetic acid, EDTA [14,15], as well as humic-like substances [16] have been employed for this purpose.



Considering the complexity of the photo-Fenton mechanism and the high number of substances that can modify the nature or amount of reactive species originated by the Fenton process, it is not surprising that recently effluents have been described, the optimum pH of which is not 2.8, but slightly above, as is the case of some food processing wastes [17].

Although there is some information on the application of photo-Fenton process to highly saline water [18–20], we think that it is interesting to gain further insight into the effect of salinity on the process at different pHs, as recently good performance of mild photo-Fenton in solutions with high concentrations of salts has been detected [21,22]. As both processes might be ruled by changes in the coordination sphere of iron, some cross-effect between changes in the concentration of  $\text{Cl}^-$  and  $\text{OH}^-$  are expected and, as far as we know, there is no work devoted to clarifying this issue. For this purpose, solar simulated reactions have been performed at acidic and mildly acidic pH using matrices with different salinity (in terms of chloride amounts). A mixture of six CECs with different structures and properties have been employed to set the efficiency of photo-Fenton in each condition. The set of CECs consists of a pesticide (acetamiprid, ACP), an antipyretic drug (acetaminophen, ACT), a stimulant (caffeine, CAF), an antibiotic (amoxicillin, AMOX), a metabolite of a lipidic regulator (clofibric acid, CLOF) and a psychiatric drug (carbamazepine, CBZ), whose structures and uses can be seen in Figure 1. This mixture of pollutants has been chosen in previous works dealing with photo-oxidation at mild pHs because of its environmental relevance and the different responses they show towards reactive species and reaction conditions [23–25].

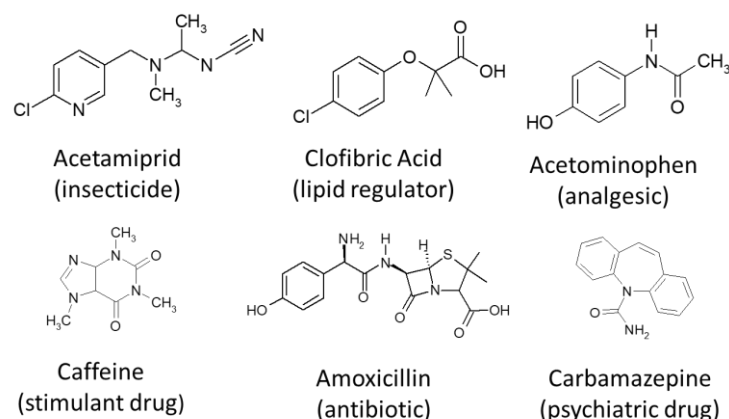


**Figure 1.** Scheme of the 6 different contaminants of emerging concern employed in this work as target pollutants.

## 2. Materials and Methods

### 2.1. Reagents

High purity (>98%) acetamiprid, acetaminophen, caffeine, amoxicillin, clofibric acid and carbamazepine, used as target pollutants, were supplied by Sigma-Aldrich (St. Louis, MO, USA). Other reagents, such as iron (II) sulfate ( $\text{FeSO}_4 \cdot 7\text{H}_2\text{O}$ ), hydrogen peroxide (30% *w/w*), sodium hydroxide, sulfuric acid and NaCl (99%) were purchased from Panreac. Water employed in all solutions was Milli-Q grade. Methanol, formic acid and acetonitrile were used as eluents for HPLC analyses, purchased from Panreac.

### 2.2. Target Solution and Water Matrices

The target solution consisted of a mixture of the six abovementioned CECs, with an initial concentration  $5 \text{ mg} \cdot \text{L}^{-1}$  of each pollutant. This initial concentration is well above that observed in seawater (typically  $\text{ng L}^{-1}$ , which accounts for a total concentration of some  $\mu\text{g L}^{-1}$ ) [26] but it ensures obtaining reliable time-resolved profiles in order to allow an accurate comparison of the different processes and reactions, which is the real goal of this paper.

Three different water matrices were used as aqueous solutions, which are defined according to their different salinities (in terms of chloride concentration): (a) distilled water (DW), (b) low-salinity water (LSW), obtained upon addition of  $1 \text{ g} \cdot \text{L}^{-1}$  of NaCl to DW (representing the chloride amount similar to brackish water) and (c) high-salinity water (HSW), which was prepared by adding  $30 \text{ g} \cdot \text{L}^{-1}$  of NaCl to DW (an amount of salt similar to seawater). The temperature did not exceed  $30 \text{ }^\circ\text{C}$  during all of the experiments.

Additionally, experiments were performed with real seawater (SW) sampled from the coast of the Mediterranean Sea in Campello, close to Alicante (East Spain). Briefly, the salinity was ca.  $36.5 \text{ g L}^{-1}$  (expressed as NaCl concentration). Diluted seawater (DSW) was prepared by diluting this sample with distilled water to reach a similar conductivity to that of LSW ( $[\text{NaCl}] = 1 \text{ g} \cdot \text{L}^{-1}$ ).

### 2.3. Experimental Set-Up

Experiments were performed in cylindrical open glass reactors (see supplementary information for a picture of the experimental set-up). The reactor was loaded with 250 mL of aqueous solution containing the six CECs. All systems were tested with  $5 \text{ mg} \cdot \text{L}^{-1}$  of iron according to previous studies [27]. The stoichiometric amount of hydrogen peroxide to mineralize the mixture of CEC was added ( $146 \text{ mg} \cdot \text{L}^{-1}$ ). This amount was chosen to set a constant initial amount of  $\text{H}_2\text{O}_2$  for all experiments and to avoid reaction interruption because of the exhaustion of  $\text{H}_2\text{O}_2$  [27]. The pH was set at the desired value for experimentation (pH = 5.0, 2.8 or 3.5) by addition of sulfuric acid or sodium hydroxide. Accordingly,

the efficiency of photo-Fenton process for the abatement of 6 different CECs were assessed in (i) different aqueous solutions with varying salinity and (ii) at different pH.

A solar simulator (Abet technologies, Milford, CT, USA, Sun 2000) equipped with a 1050 W xenon lamp was employed to irradiate the open glass reactor. Borosilicate glass filters were employed to cut off wavelengths  $\lambda < 300$  nm. Irradiation for each experiment was carried out for up to one hour. Samples were periodically taken from the solution and diluted 1:0.4 with methanol in order to quench the remaining hydrogen peroxide and, consequently, to stop the Fenton reaction.

#### 2.4. Analytical Measurements

The concentration of each CEC was determined by a HPLC (Hitachi Chromaster chromatograph; VWR) with a Chromaster System Manager (v1.1). A Prevail Hichrom column (C18-Select;  $250 \times 4.6$  mm;  $5 \mu\text{m}$ ) was employed as a stationary phase. The mobile phase was a binary mixture of A (acetonitrile) and B (10 mM formic acid aqueous solution). The linear gradient was operated from 10% A to 90% A in 25 min. Re-equilibration time was 7 min. A flow rate of  $1 \text{ mL} \cdot \text{min}^{-1}$  was used. The wavelength used for the quantification of the CECs was 225 nm. Errors associated with HPLC analysis were systematically below 5%.

The concentration of hydrogen peroxide was determined according to the colorimetric method based on metavanadate, which can be found in detail elsewhere [28], and iron was monitored according to the o-phenantroline standard method (ISO 6332).

Data was analyzed by means of time-response curves. Normalized concentrations ( $C/C_0$ ) versus time were obtained for each CEC and for each system evaluated. For simplicity of interpretation of the results, the sum of the total CECs investigated was represented.

### 3. Results

#### 3.1. Interference of Chlorides and pH on the Photo-Fenton Process

The photo-Fenton process was first applied to remove a mixture of the six CECs at pH = 5 in three different matrices (DW, LSW and HSW). Plots of the relative concentration of each pollutant vs. irradiation time are shown in Figure 2.

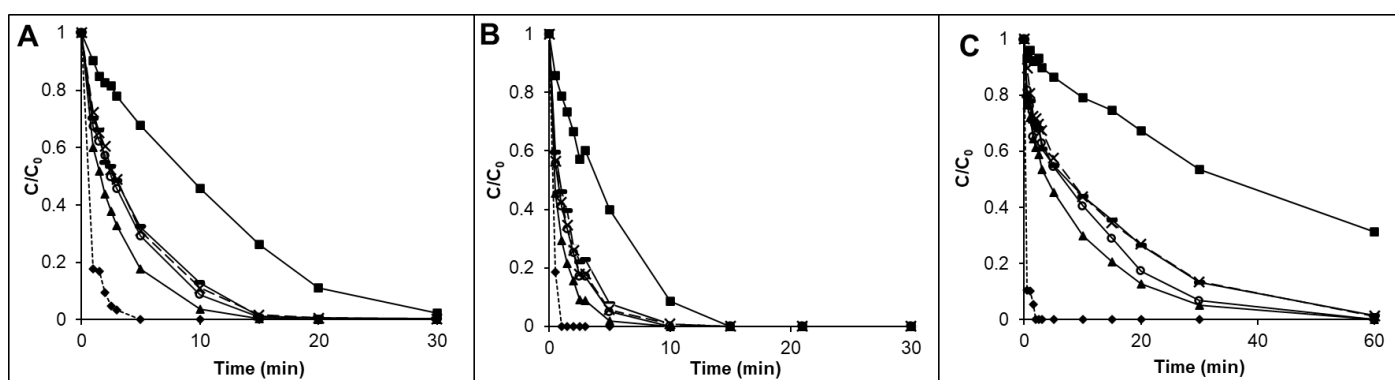


**Figure 2.** Photo-Fenton treatment of a mixture of pollutants at pH 5 in solutions containing different concentrations of salt: (A). DW, (B). LSW and (C). HSW. Plot of the relative concentration of each pollutant vs. time: (◆) amoxicillin, (-) acetaminophen, (■) acetamidrid, (○) clofibric acid, (×) caffeine, (▲) carbamazepine.

It can be observed that, systematically, amoxicillin showed the fastest degradation, most probably due to its complex structure, which contains a high number of sites that can be attached by the reactive species. Acetamidrid seems to be the most reluctant towards this process, because of the low reactivity of the pyridine ring vs. the electrophilic reactive species. The other four pollutants (CLOF, CAF, CBZ, ACT) follow similar kinetics and the order of reactivity is not influenced by the water matrices.

More interesting are the different behaviors that they exhibit in the studied water matrices. A first sight to Figure 2A–C shows that the efficiency of photo-Fenton varies according to the series LSW > DW > HSW. In order to see this effect more clearly, the relative total amount of the total concentration of emerging pollutants,  $\Sigma\text{CECs}$  ( $C/C_0$ ), are shown in Figure 3. Data confirms the trends indicated, namely, that the presence of  $1\text{ g}\cdot\text{L}^{-1}$  of NaCl was able to enhance photo-Fenton, when compared with DW, while higher NaCl concentrations (HSW) are detrimental for the removal of CECs. However, it is noteworthy indicating that even photo-Fenton in HSW is much faster than Fenton in distilled water.

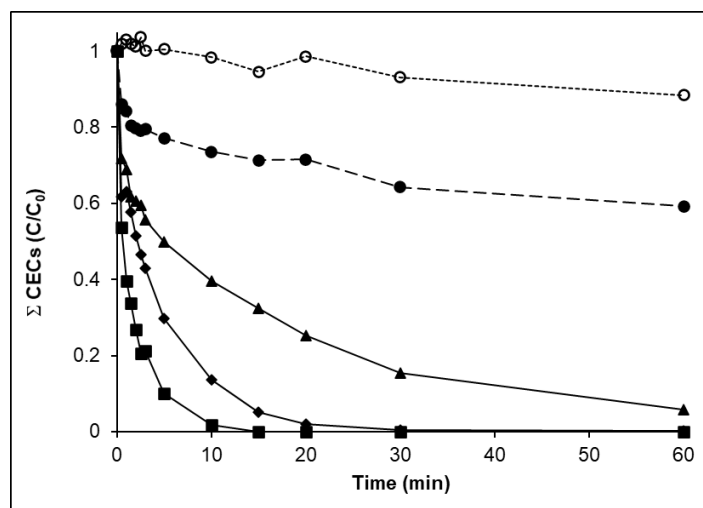


**Figure 3.** Photo-Fenton treatment of a mixture of pollutants at pH = 5 under different conditions: DW (◆), LSW (■) and HSW (▲). Results obtained for Fenton (●) and photolysis (○) in DW are also given for comparison. Plots of the relative amount of the total concentration of emerging pollutants,  $\Sigma\text{CECs}$  ( $C/C_0$ ) vs. time are given.

These results are in sharp contrast with the fact that most papers report that chlorides have a strong negative effect on the Fenton process [9,15,20,29], although it has been recently reported that relatively low concentrations of chlorides can enhance disinfection by photo-Fenton [30]. This effect can be associated to modifications in the coordination sphere of  $\text{Fe}^{3+}$ , which result in changes in the mechanism, in which species such as  $\text{Fe}(\text{Cl})^{2+}$  play a very important role [29,31]. Hence, the reaction (4) competes with reaction (2), finally generating  $\text{Cl}_2^{\cdot-}$  radicals in the presence of  $\text{Cl}^-$  according to reaction (5). Although this chlorinated species can react with some molecules, it is not as reactive and unselective as  $\cdot\text{OH}$  [32].



An additional process that might occur is the scavenging effect of  $\text{Cl}^-$  towards hydroxyl radicals ( $k \approx 10^9\text{ M}^{-1}\cdot\text{s}^{-1}$ ), also to generate  $\text{Cl}^{\cdot}$  or  $\text{Cl}_2^{\cdot-}$  (Equation (6)), a process that is more important in an acidic medium [9,29].



However, it has to be considered that this slight acceleration of photo-Fenton in the presence of  $1\text{ g}\cdot\text{L}^{-1}$  of chlorides occurs at pH = 5, in contrast with the pH below 3 that was used in most of the experiments reported in literature. As a matter of fact, results obtained at pH = 2.8 in different aqueous matrices shows that the expected trend is obtained and lower reaction rate is observed at  $1\text{ g}\cdot\text{L}^{-1}$  when compared with distilled water (Figure 4). In order to explain this behavior, it has to be considered that  $\text{OH}^-$  shows higher affinity for iron than  $\text{Cl}^-$ , and only when  $[\text{Cl}^-]$  is well above  $[\text{OH}^-]$  chlorinated complexes are formed,

namely at acidic pH. This means that in the presence of chlorides the highest concentration of  $\text{Fe}(\text{OH})^{2+}$  is no longer reached at  $\text{pH} = 2.8$ , but it is shifted towards higher pH values, as reported by Millero [33].

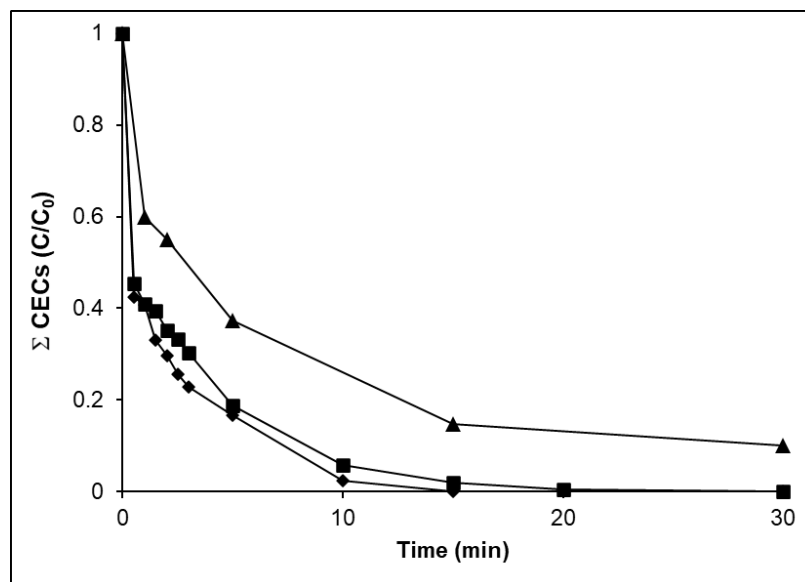


**Figure 4.** Photo-Fenton treatment of a mixture of pollutants at  $\text{pH} = 2.8$  under different conditions: DW (◆), LSW (■), and HSW (▲). Plots of the relative amount of the total concentration of emerging pollutants,  $\Sigma \text{CECs} (C/C_0)$  vs. time are given.

The pH dependence of photo-Fenton in the presence of moderate concentrations of chlorides has been previously reported in a couple of works [7,29]. It was reported that the inhibitory effect of chlorides was very strong at  $\text{pH} < 3$ , while it decreased at higher pH values; hence, the optimum pH condition shifted towards higher values. In order to clarify this point, the experiment with  $1 \text{ g L}^{-1}$  of NaCl was run at  $\text{pH} = 3.5$ ; thus, Figure 5 shows that the reaction was faster than at the other studied pH. It is worth indicating that in our case, the pH of reactions performed at  $\text{pH} = 5$  decreases to values around 4 in the early stages of the reactions, thus approaching the optimum value.

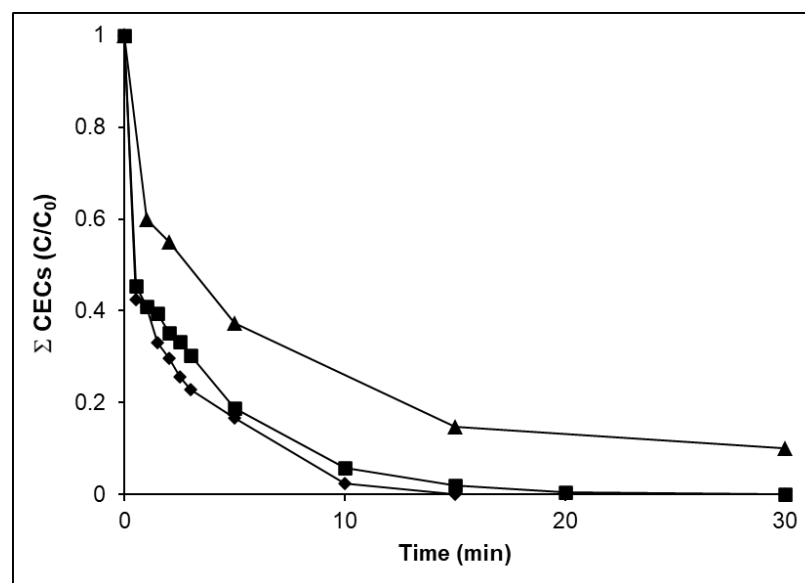


**Figure 5.** Photo-Fenton treatment of a mixture of pollutants in LSW at three different pH values: 2.8 (◆), 3.5 (●), and 5.0 (▲). Plot of the  $\Sigma \text{CEC}/\Sigma \text{CEC}_0$  vs. time.

### 3.2. Evolution of pH, Dissolved Iron and Hydrogen Peroxide in Photo-Fenton Reactions

In order to gain further insight into the differences in the tested experimental conditions, pH, dissolved iron and hydrogen peroxide were also tested during the experiments. Regarding pH, no noticeable changes were found when experiments were performed at pH = 2.8, while at pH = 5, a fast decrease was observed in the first 15 min to reach values around 4, and then remained nearly constant. Regarding iron and H<sub>2</sub>O<sub>2</sub>, the remaining percentages of these substances in solution after 15 min and 60 min are shown in Table 1. The amount of dissolved iron remained constant in experiments at pH = 2.8, while, in contrast, a decrease in dissolved iron was observed at pH = 5.0 as a consequence of the formation of non-soluble iron oxides and hydroxides, which is favored at mildly acidic or neutral pH and responsible for iron inactivation, as stated above. In HSW, higher amounts of iron remained in the solution after 60 min (77% vs. ca. 20% in DW and LSW), which can be attributed to some stabilization because of the presence of chlorides.

**Table 1.** Remaining percentages of H<sub>2</sub>O<sub>2</sub> and dissolved iron after 15 min or 60 min of irradiation time. Experiments performed at pH 5 or pH 2.8 for DW, LSW and HSW aqueous matrices.

		t = 15 min		t = 60 min	
		Remaining H <sub>2</sub> O <sub>2</sub> (%)	Remaining Fe (%)	Remaining H <sub>2</sub> O <sub>2</sub> (%)	Remaining Fe (%)
pH = 5	DW	51	76	11	16
	LSW	55	73	11	22
	HSW	77	95	42	77
pH = 2.8	DW	35	99	0	99
	LSW	57	98	4	97
	HSW	69	100	10	99

On the other hand, hydrogen peroxide consumption is not completely ruled either by pH or by dissolved iron, and it is correlated with the efficiency of photo-Fenton. An experiment at pH = 2.8 in DW resulted in complete consumption of H<sub>2</sub>O<sub>2</sub> and resulted in the best performance of photo-Fenton. The remaining amount of hydrogen peroxide after 15 min was in the range 51–57% for LSW at pH = 2.8 and DW or LSW at pH = 5. This is in line with observations that chlorides interfered at pH = 2.8 but not at pH = 5. It is also worth indicating that the consumption of H<sub>2</sub>O<sub>2</sub> remained relatively high at pH = 5 despite the lower amount of iron in solution, indicating that dissolved iron was in an active form for photo-Fenton. In sharp contrast, with a high concentration of salt, iron was not able to decompose H<sub>2</sub>O<sub>2</sub> efficiently despite the presence of high amounts of iron, being the reaction faster at pH = 2.8. This effect might mean that high concentrations of chlorides do not inhibit photo-Fenton by formation of non-soluble oxygenated species, but by generation of inefficient chlorinated complexes, which prevent reaction of iron salts with H<sub>2</sub>O<sub>2</sub>.

### 3.3. Experiments with Real/Natural Aqueous Matrix

Data show that photo-Fenton in HSW was clearly less efficient than in the other matrices, both at pH = 2.8 and pH = 5.0., although under those conditions, complete removal of all six pollutants could be accomplished after 1 h of treatment. As this concentration of chlorides is close to that of the Mediterranean Sea (36–37 g L<sup>-1</sup>), it seemed interesting to repeat the experiments with real seawater (SW). Figure 6 indicates that the performance vs. photo-Fenton was worse at pH = 2.8 (Figure 6A) and, in particular, at pH = 5, when compared with HSW (Figure 6B). This is probably due to the presence of other species in SW, which is more complex than merely a NaCl solution. Some anions such as bromides are candidates to explain this effect, but other species such as dissolved organic matter or suspended solids can also contribute. Finally, in order to see what occurred at low salinity levels, “diluted

sea water" (DSW) was prepared by diluting SW to reach the same conductivity as  $1 \text{ g L}^{-1}$  of NaCl. Figure 6 shows that also in this case a slight loss of efficiency was detected when compared with LSW, although a good performance was still found.

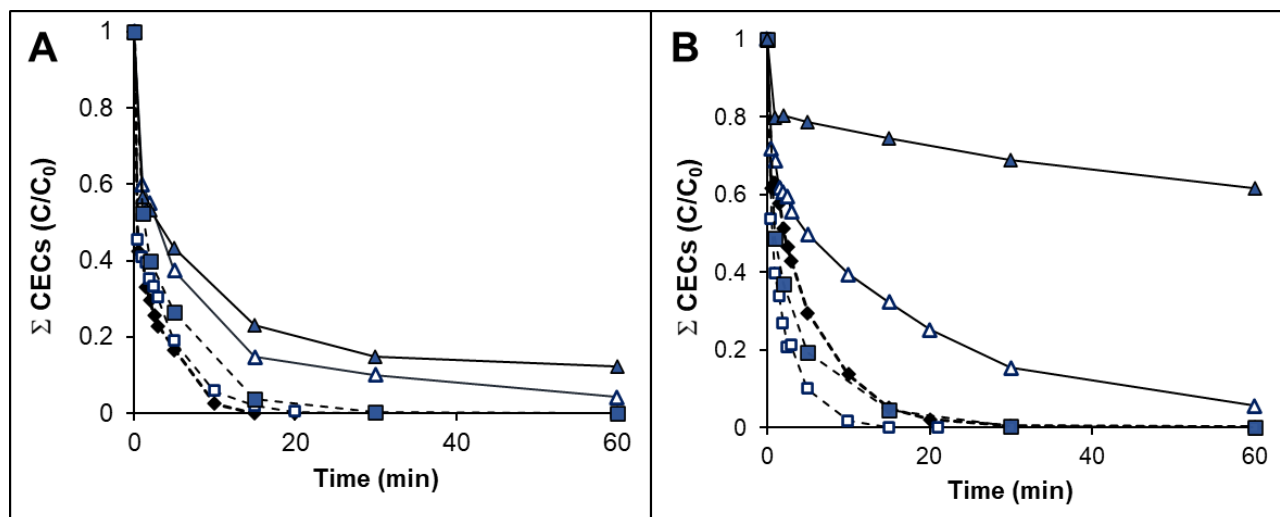


**Figure 6.** Photo-Fenton treatment of a mixture of pollutants at (A). pH 2.8 and (B). pH 5 in different aqueous matrices DW (◆), DSW (■), LSW (□), SW (▲) and HSW (△). Plot of the  $\Sigma \text{CEC} / \Sigma \text{CEC}_0$  vs. time.

#### 4. Conclusions

The effect of the presence of chlorides on the photo-Fenton process depends on pH; while at pH = 2.8 chlorides are always detrimental, at pH = 5 a slight acceleration can be observed at  $1 \text{ g} \cdot \text{L}^{-1}$ , which can be associated to a shift of  $\text{Fe}(\text{OH})_2$  formation towards higher pH values. As a matter of fact, higher efficiency of photo-Fenton was obtained at pH = 3.5 in agreement with literature. Hydrogen peroxide consumption and dissolved iron indicate that chloride interferences are due to changes in the coordination sphere of iron, rather than to the scavenging effect of iron towards the hydroxyl radical.

The difference in reactivity between SW and HSW should be attributable to other species that are present in the medium and systematic studies to determine the role of each species, pH dependence and mechanism are required. Furthermore, in order to determine the real applicability, complementary experiments would be required, not only focusing on the primary degradation of the pollutants, but also on monitoring changes in biocompatibility, release of reaction intermediates and changes in the composition of the organic fraction of the effluent.

**Author Contributions:** Conceptualization, J.M.-A. and A.M.A.; methodology, J.M.-A., L.S.-J. and A.A.; validation, J.M.-A., L.S.-J. and A.A.; formal analysis, J.M.-A., A.A.; investigation, J.M.-A., I.V.; resources, A.A.; data curation, J.M.-A., I.V.; writing—original draft preparation, J.M.-A. and A.A.; writing—review and editing, J.M.-A., L.S.-J., and A.A.; visualization, J.M.-A. and A.A.; supervision, A.A.; project administration, A.A.; funding acquisition, J.M.-A. and A.M.A. All authors have read and agreed to the published version of the manuscript.

**Funding:** This research was funded by Spanish Ministry of Science, Innovation and Universities, AEI and FEDER for funding under the CalypSol Project (Ref: RTI2018- 097997-B-C31) and the co-funding by the 2014–2020 ERDF Operational Programme and by the Department of Economy, Knowledge, Business and University of the Regional Government of Andalusia (Spain). Ref.: FEDER-UCA18-108023. J. Moreno-Andrés is grateful to Generalitat Valenciana (Spain) (APOSTD/2019/207) and the financial support from the European Social Fund (ESF).

**Institutional Review Board Statement:** Not applicable.

**Informed Consent Statement:** Not applicable.



**Data Availability Statement:** Not applicable.

**Conflicts of Interest:** The authors declare no conflict of interest.

## References

1. Wolfram, J.; Stehle, S.; Bub, S.; Petschick, L.L.; Schulz, R. Water quality and ecological risks in European surface waters—Monitoring improves while water quality decreases. *Environ. Int.* **2021**, *152*, 106479. [[CrossRef](#)]
2. Patel, M.; Kumar, R.; Kishor, K.; Mlsna, T.; Pittman, C.U.; Mohan, D. Pharmaceuticals of emerging concern in aquatic systems: Chemistry, occurrence, effects, and removal methods. *Chem. Rev.* **2019**, *119*, 3510–3673. [[CrossRef](#)]
3. Cuerda-Correa, E.M.; Alexandre-Franco, M.F.; Fernández-González, C. Advanced oxidation processes for the removal of antibiotics from water. An overview. *Water* **2020**, *12*, 102. [[CrossRef](#)]
4. Pignatello, J.J.; Oliveros, E.; MacKay, A. Advanced oxidation processes for organic contaminant destruction based on the Fenton reaction and related chemistry. *Crit. Rev. Environ. Sci. Technol.* **2006**, *36*, 1–84. [[CrossRef](#)]
5. Malato, S.; Fernández-Ibáñez, P.; Maldonado, M.I.; Blanco, J.; Gernjak, W. Decontamination and disinfection of water by solar photocatalysis: Recent overview and trends. *Catal. Today* **2009**, *147*, 1–59. [[CrossRef](#)]
6. Santos-Juanes, L.; Amat, A.M.; Arques, A. Strategies to drive photo-Fenton process at mild conditions for the removal of xenobiotics from aqueous systems. *Curr. Org. Chem.* **2017**, *21*, 1074–1083. [[CrossRef](#)]
7. Soler, J.; García-Ripoll, A.; Hayek, N.; Miró, P.; Vicente, R.; Arques, A.; Amat, A.M. Effect of inorganic ions on the solar detoxification of water polluted with pesticides. *Water Res.* **2009**, *43*, 4441–4450. [[CrossRef](#)]
8. Micó, M.M.; Zapata, A.; Maldonado, M.I.; Bacardit, J.; Malfeito, J.; Sans, C. Fosetyl-Al photo-Fenton degradation and its endogenous catalyst inhibition. *J. Hazard. Mater.* **2014**, *265*, 177–184. [[CrossRef](#)] [[PubMed](#)]
9. De, L.J.; Giang, L.T. Effects of chloride ions on the iron(III)-catalyzed decomposition of hydrogen peroxide and on the efficiency of the Fenton-like oxidation process. *Appl. Catal. B Environ.* **2006**, *66*, 137–146.
10. Santos da Silva, S.; Chiavone-Filho, O.; Neto, E.L.B.; Foletto, E.L.; Mota, A.L.N. Effect of inorganic salt mixtures on phenol mineralization by photo-Fenton—Analysis via an experimental design. *Water Air Soil Pollut.* **2014**, *225*, 1784. [[CrossRef](#)]
11. Patra, S.G.; Mizrahi, A.; Meyerstein, D. The role of carbonate in catalytic oxidations. *Acc. Chem. Res.* **2020**, *53*, 2189–2200. [[CrossRef](#)] [[PubMed](#)]
12. Souza, B.M.; Dezotti, M.W.C.; Boaventura, R.A.R.; Vilar, V.J.P. Intensification of a solar photo-Fenton reaction at near neutral pH with ferrioxalate complexes: A case study on diclofenac removal from aqueous solutions. *Chem. Eng. J.* **2014**, *256*, 448–457. [[CrossRef](#)]
13. Zhou, H.; Zhang, H.; He, Y.; Huang, B.; Zhou, C.; Yao, G.; Lai, B. Critical review of reductant-enhanced peroxide activation processes: Trade-off between accelerated  $\text{Fe}^{3+}/\text{Fe}^{2+}$  cycle and quenching reactions. *Appl. Catal. B Environ.* **2021**, *286*, 119900. [[CrossRef](#)]
14. Huang, W.; Brigante, M.; Wu, F.; Hanna, K.; Mailhot, G. Development of a new homogenous photo-Fenton process using Fe(III)-EDDS complexes. *J. Photochem. Photobiol. A* **2012**, *239*, 17–23. [[CrossRef](#)]
15. Klammerth, N.; Malato, S.; Agüera, A.; Fernández-Alba, A.; Mailhot, G. Treatment of municipal wastewater treatment plant effluents with modified photo-Fenton as a tertiary treatment for the degradation of micro pollutants and disinfection. *Environ. Sci. Technol.* **2012**, *46*, 2885–2892. [[CrossRef](#)]
16. Gomis, J.; Bianco Prevot, A.; Montoneri, E.; González, M.C.; Amat, A.M.; Mártire, D.O.; Arques, A.; Carlos, L. Waste sourced bio-based substances for solar-driven wastewater remediation: Photodegradation of emerging pollutants. *Chem. Eng. J.* **2014**, *235*, 236–243. [[CrossRef](#)]
17. García-Ballesteros, S.; Mora, M.; Vicente, R.; Sabater, C.; Castillo, M.A.; Arques, A.; Amat, A.M. Gaining further insight into photo-Fenton treatment of phenolic compounds commonly found in food processing industry. *Chem. Eng. J.* **2016**, *288*, 126–136. [[CrossRef](#)]
18. Maciel, R.; Sant’Anna, G.L., Jr.; Dezotti, M. Phenol removal from high salinity effluents using Fenton’s reagent and photo-Fenton reactions. *Chemosphere* **2004**, *57*, 711–719. [[CrossRef](#)]
19. Moraes, J.E.F.; Quina, F.H.; Nascimento, C.A.O.; Silva, D.N.; Chiavone-Filho, O. Treatment of saline wastewater contaminated with hydrocarbons by the photo-Fenton process. *Environ. Sci. Technol.* **2004**, *38*, 1183–1187. [[CrossRef](#)]
20. Bacardit, J.; Stoltzner, J.; Chamarro, E.; Esplugas, S. Effect of salinity on the photo-Fenton process. *Ind. Eng. Chem. Res.* **2007**, *46*, 7615–7619. [[CrossRef](#)]
21. Deemter, D.; Oller, I.; Amat, A.M.; Malato, S. Effect of salinity on preconcentration of contaminants of emerging concern by nanofiltration: Application of solar photo-Fenton as a tertiary treatment. *Sci. Total Environ.* **2021**, *756*, 143593. [[CrossRef](#)]
22. Sciscenko, I.; Garcia-Ballesteros, S.; Sabater, C.; Castillo, M.A.; Escudero-Oñate, C.; Oller, I.; Arques, A. Monitoring photolysis and (solar photo)-Fenton of enrofloxacin by a methodology involving EEM-PARAFAC and bioassays: Role of pH and water matrix. *Sci. Total Environ.* **2020**, *719*, 137331. [[CrossRef](#)] [[PubMed](#)]
23. Carlos, L.; Mártire, D.O.; Gonzalez, M.C.; Gomis, J.; Bernabeu, A.; Amat, A.M.; Arques, A. Photochemical fate of a mixture of emerging pollutants in the presence of humic substances. *Water Res.* **2012**, *46*, 4732–4740. [[CrossRef](#)]
24. Gomis, J.; Gonçalves, M.G.; Vercher, R.F.; Sabater, C.; Castillo, M.A.; Bianco Prevot, A.; Amat, A.M.; Arques, A. Determination of photostability, biocompatibility and efficiency as photo-Fenton auxiliaries of three different types of soluble bio-based substances (SBO). *Catal. Today* **2015**, *252*, 177–183. [[CrossRef](#)]

25. Moreno-Andrés, J.; Vallés, I.; García-Negueroles, P.; Santos-Juanes, L.; Arques, A. Enhancement of iron-based photo-driven processes by the presence of catechol moieties. *Catalysts* **2021**, *11*, 372. [[CrossRef](#)]
26. Brumovský, M.; Bečanová, J.; Kohoutek, J.; Borghini, M.; Nizzetto, L. Contaminants of emerging concern in the open sea waters of the Western Mediterranean. *Environ. Pollut.* **2017**, *229*, 976–983. [[CrossRef](#)] [[PubMed](#)]
27. Gomis, J.; Carlos, L.; Bianco Prevot, A.; Teixeira, A.C.S.C.; Mora, M.; Amat, A.M.; Vicente, R.; Arques, A. Bio-based substances from urban waste as auxiliaries for solar photo-Fenton treatment under mild conditions: Optimization of operational variables. *Catal. Today* **2015**, *240*, 39–45. [[CrossRef](#)]
28. Nogueira, R.F.P.; Oliveira, M.C.; Paterlini, W.C. Simple and fast spectrophotometric determination of H<sub>2</sub>O<sub>2</sub> in photo-Fenton reactions using metavanadate. *Talanta* **2005**, *66*, 86–91. [[CrossRef](#)] [[PubMed](#)]
29. Machulek, A.J.; Moraes, J.E.; Vautier-Giongo, C.; Silverio, C.A.; Friedrich, L.C.; Nascimento, C.A.; Gonzalez, M.C.; Quina, F.H. Abatement of the inhibitory effect of chloride anions on the photo-Fenton process. *Environ. Sci. Technol.* **2007**, *41*, 8459–8463. [[CrossRef](#)]
30. Rommozzi, E.; Giannakis, S.; Giovannetti, R.; Vione, D.; Pulgarin, C. Detrimental vs. beneficial influence of ions during solar (SODIS) and photo-Fenton disinfection of *E. coli* in water: (bi)carbonate, chloride, nitrate and nitrite effects. *Appl. Catal. B Environ.* **2020**, *270*, 118877. [[CrossRef](#)]
31. Machulek, A., Jr.; Vautier-Giongo, C.; Moraes, J.E.F.; Nascimento, C.A.O.; Quina, F.H. Laser flash photolysis study of the photocatalytic step of the photo-Fenton reaction in saline solution. *Photochem. Photobiol.* **2006**, *82*, 208–212. [[CrossRef](#)] [[PubMed](#)]
32. Caregnato, P.; Rosso, J.A.; Soler, J.M.; Arques, A.; Martire, D.O.; González, M.C. Chloride anion effect on the advanced oxidation process of methidathion and dimethoate: Role of C<sub>12</sub>•<sup>-</sup> radical. *Water Res.* **2013**, *47*, 351–362. [[CrossRef](#)] [[PubMed](#)]
33. Millero, F.J. Solubility of Fe III in seawater. *Earth Planet. Sci. Lett.* **1999**, *154*, 323–329. [[CrossRef](#)]